Eur. Phys. J. A **3**, 255–262 (1998)

THE EUROPEAN PHYSICAL JOURNAL A

Pseudo-spin as a relativistic symmetry

Y.K. Gambhir, J.P. Maharana, C.S. Warke

Department of Physics, Indian Institute of Technology Bombay, Powai, Mumbai, 400 076, INDIA

Received: 16 April 1998 / Revised version: 26 June 1998
Communicated by P. Schuck

Abstract. The existence of broken pseudo-spin symmetry in the Pb nucleus has been studied in the relativistic mean field approach using realistic Lagrangian parameters. Its relationship to spin orbit splitting and the vanishingly small surface delta character of the mean spin orbit potential are investigated. In the ^{208}Pb nucleus the broken pseudo-spin doublets are found to exist above the neutron (proton) Fermi surfaces.

PACS. 21.60.Cs Shell model – 21.10.-k Properties of nuclei; nuclei energy levels – 21.30 Nuclear forces

1 Introduction

In the light and heavy near spherical mass region of nuclei it has been observed that the pair of normal parity orbitals $(n,\ \ell,\ j = \ell + \frac{1}{2})$ and $(n-1,\ \ell+2,\ j = \ell + \frac{3}{2}$ in the major shells are nearly degenerate [1–4]. This observed quasidegeneracy implies a symmetry called broken pseudo-spin symmetry. Since j^π are conserved quantum numbers for a nucleus, the pseudo angular momenta $(\tilde{\ell},\ \tilde{s})$ satisfy $\mathbf{j} = \tilde{\ell} + \tilde{\mathbf{s}}$. In order to interpret this near degenerate pair of $j = \ell + 1/2$ and $j = \ell + 3/2$ as pseudo-spin multiplets corresponding to $j = \tilde{\ell} \pm 1/2$, $\tilde{\ell}$ has to be $\ell+1$. In the case of highly deformed heavy nuclei, pseudo-spin orbit interaction is weak and the asymptotic Nilsson pseudo-angular quantum numbers $(\underline{N}n_{\underline{z}}, \underline{\Lambda}, \underline{\Omega})$ would be valid and $\underline{\Omega} = \underline{\Lambda} \pm 1/2$ orbitals would be degenerate. The implications of the pseudo-spin degeneracy is the existence of nuclear degenerate rotational bands based on these intrinsic orbitals as observed in super deformed nuclei [4]. The early quantitative work in this mass region has been based on the pseudo SU(3) model developed by Ratna Raju *et al* [5]. The pseudo-spin symmetry is incorporated in this model. Nuclear many body techniques are evolved in search of suitable approximation schemes by transforming a given Hamiltonian using the pseudo-spin transformations [6–9]. The existence of such a transformation operator was first dealt with in [3] and was explicitly developed for Nilsson type Hamiltonian. These models were used successfully for the description of several nuclear properties for the past twenty years. Among the recent such non-relativistic developments are in [10,11]. Blokhin *et al* [8,10] devised the approximate pseudo-spin transformation operator from the projection of the momentum helicity states on to the oscillator states for arbitrary nuclear shapes. It simplifies the microscopic many body calculations of heavy nuclei. The transformation technique is useful in understanding the origin of the pseudo-spin symmetry and in finding out, how good the symmetry is. It is expected that in the presence of two nucleon interaction and deformed nuclear shape pseudo-spin symmetry may be destroyed. These quantitative investigations reveal that this symmetry is only slightly broken in the realistic many body calculations [10,11]. It validates the single particle and many particle pseudo-spin models.

In a recent paper [12] the author conjectured the origin of pseudo-spin symmetry as due to near equality in magnitude of the attractive scalar σ and repulsive ω relativistic mean fields. In the present paper we check its validity within the Relativistic Mean Field (RMF) approach that reproduces the other observed ground state properties of nuclei. The difference in the radial wave functions of the pseudo-spin doublets, the relationships of pseudo-spin symmetry to the spin orbit coupling strength and possible surface delta interaction structure and the behaviour of the root mean square radii are also studied. In order to find out its relationship to the nuclear interactions, the variation of the pseudo-spin doublet splitting with the relative strengths of scalar and vector fields is investigated. Wherever possible qualitative arguments are presented to explain the results.

A brief description of RMF approximation and the relevant Lagrangian parameters are given in Sec. 2. Interpretation of the numerical results in terms of pseudo-spin symmetry is contained in Sec. 3. Some analytic properties are discussed in Sec. 4. The last Sec. 5, summarises the results.

Correspondence to: yogy@niharika.phy.iitb.ernet.in, jyoti@niharika.phy.iitb.ernet.in

2 Relativistic mean field approximation

A brief review of the RMF approximation is in order here. The classical mean fields, scalar σ and vector ω are produced by the relativistic nucleon sources. The Lagrangian density describing their dynamics is taken to be that considered by Walecka [13] (in the notations of [14]).

$$L \;=\; L_{free} + L_{int}\;; \tag{1}$$

with

$$L_{free} \;=\; L_{B_{free}} + L_{M_{free}} \quad . \tag{2}$$

The free baryonic part is given by

$$L_{B_{free}} \;=\; \bar{\psi}\,(i\gamma^{\mu}\partial_{\mu} \;-\; M)\,\psi\;; \tag{3}$$

and the mesonic part

$$\begin{aligned} L_{M_{free}} \;=\;& \frac{1}{2}\partial^{\mu}\sigma\partial_{\mu}\sigma \\ & - \frac{1}{2}{m_{\sigma}}^{2}\sigma^{2} \;-\; \frac{1}{3}g_{2}\sigma^{3} \;-\; \frac{1}{4}g_{3}\sigma^{4} \\ & - \frac{1}{4}\mathbf{\Omega}^{\mu\nu}\mathbf{\Omega}_{\mu\nu} \;+\; \frac{1}{2}m_{\omega}^{2}\omega^{\mu}\omega_{\mu} \quad . \end{aligned} \tag{4}$$

The interaction part with the minimal coupling is

$$\begin{aligned} L_{int} \;=\;& -\,g_{\sigma}\bar{\psi}_{i}\psi_{i}\sigma \\ & -\,g_{\omega}\bar{\psi}_{i}\gamma^{\mu}\psi_{i}\omega_{\mu} \quad . \end{aligned} \tag{5}$$

Here $\Omega_{\mu\nu} = \partial^{\mu}\omega^{\nu} - \partial^{\nu}\omega^{\mu}$.

The variational nuclear many body wavefunction is a Slater determinant of Dirac spinors. Since the exchange contributions are neglected, the Hartree-approximation is implied in the nucleon sector. The nucleus under consideration is assumed to be spherical and its wavefunction is assumed to be consistent with charge and time reversal symmetry invariant. The variational approach then leads to the following equations for the bound Dirac single particle orbitals and the classical meson fields.

$$\big\{\alpha(-\imath\nabla) + \beta M(\mathbf{r}) + V(\mathbf{r})\big\}\psi_{i}(\mathbf{r}) = \;\epsilon_{i}\;\psi_{i}(\mathbf{r}) \quad . \tag{6}$$

$$\begin{aligned} \big\{-\mathbf{\Delta} \;+\; m_{\sigma}^{2}\big\}\,\sigma(\mathbf{r}) \;&=-g_{\sigma}\rho_{s}(\mathbf{r}) \\ &\quad -g_{2}\sigma^{2}(\mathbf{r}) \;-\; g_{3}\sigma^{3}(\mathbf{r}) \quad . \end{aligned} \tag{7}$$

$$\big\{\;-\mathbf{\Delta} \;+\; m_{\omega}^{2}\big\}\,\omega^{0}(\mathbf{r}) \;=-g_{\omega}\rho_{v}(\mathbf{r}). \tag{8}$$

Here the potential $V(\mathbf{r})$, is given by

$$V(\mathbf{r}) \;=\; g_{\omega}\omega^{0}(\mathbf{r}) + \beta g_{\sigma}\sigma(r) \quad . \tag{9}$$

The baryon currents and densities are defined as

$$\rho_{s}(\mathbf{r}) \;=\; \sum_{i=1}^{A}\;\bar{\psi}_{i}(\mathbf{r})\psi_{i}(\mathbf{r}) \tag{10}$$

$$\rho_{v}(\mathbf{r}) \;=\; \sum_{i=1}^{A}\;{\psi_{i}}^{\dagger}(\mathbf{r})\psi_{i}(\mathbf{r}) \quad . \tag{11}$$

The sums in the definitions of densities run over the nucleon occupied orbitals only above the Dirac sea. The Dirac equation is solved using the harmonic oscillator basis expansion method for the upper and lower components.

For spherically symmetric case the nucleon spinor $\psi_{i}(\mathbf{r}, s, t)$ is chosen to be of the form

$$\begin{aligned} \psi_{i}(\mathbf{r}, s, t) &= \begin{pmatrix} \psi_{u_i} \\ \psi_{l_i} \end{pmatrix} \\ &= \begin{pmatrix} f_{i}(r)\;\Phi_{\ell_i j_i m_i}(\vartheta,\varphi,s) \\ ig_{i}(r)\;\Phi_{\tilde{\ell}_i j_i m_i}(\vartheta,\varphi,s) \end{pmatrix}\chi_{t_i}(t) \end{aligned} \tag{12}$$

with

$$\begin{aligned} &\Phi_{\ell jm}(\vartheta,\varphi,s) \\ &= \sum_{m_s m_\ell}\;\left\langle \ell m_\ell \frac{1}{2} m_s \middle| jm \right\rangle Y_{\ell m_\ell}(\vartheta,\varphi)\chi_{m_s}(s); \end{aligned} \tag{13}$$

where $Y_{\ell m_\ell}(\vartheta,\varphi)$ is the spherical harmonics and χ_{t_i} ($\chi_{ms}(s)$) is the isospin (spin) part of the wave function of the nucleon i. The orbital angular momenta ℓ_i and $\tilde{\ell}_i$ are determined by j_i and the parity π_i as

$$\ell \;=\; j + 1/2,\; \tilde{\ell} \;=\; j - 1/2 \quad \text{for} \quad \pi \;=\; (-)^{j+1/2} \tag{14}$$

and

$$\ell \;=\; j - 1/2,\; \tilde{\ell} \;=\; j + 1/2 \quad \text{for} \quad \pi \;=\; (-)^{j-1/2}. \tag{15}$$

The eigen values of the operator $-\beta(\mathbf{\Sigma}\cdot\mathbf{L} + 1)$ are denoted by κ and they are given by

$$\kappa \;=\; \mp\left(j + \frac{1}{2}\right) \qquad \text{for} \qquad j = \ell \pm \frac{1}{2}\;. \tag{16}$$

Substituting this form of ψ_i in the Dirac equation (6), one gets a coupled set of ordinary differential equations in a single variable r, for the upper (f_i) and lower (g_i) components of the Dirac spinor.

$$\begin{aligned} &(M + u(r))\,f_{i}(r) - \left(\partial_{r} - \frac{\kappa_{i} - 1}{r}\right)g_{i}(r) \\ &\qquad = \varepsilon_{i} f_{i}(r) \end{aligned} \tag{17}$$

$$\begin{aligned} &\left(\partial_{r} + \frac{\kappa_{i} + 1}{r}\right)f_{i}(r) - (M + w(r))\,g_{i}(r) \\ &\qquad = \epsilon_{i} g_{i}(r)\;. \end{aligned} \tag{18}$$

Where $u(r) = g_{\sigma}\sigma + g_{\omega}\omega$ and $w(r) = -g_{\sigma}\sigma + g_{\omega}\omega$. From now on we suppress the superscript ^{0} and use ω in place of ω^0.

For the case of non-zero eigen values far away from $E = 0$ the Dirac equation has to be solved numerically. It is solved self-consistently by an iterative method for the bound orbitals above the Dirac sea and for the corresponding eigen values for a given spherical nucleus. Here we use the NL1 set of Lagrangian parameters which successfully reproduces the ground state properties of finite nuclei over the entire periodic table [14].

3 Interpretation of results in terms of pseudo-spin symmetry

The search of pseudo-spin symmetry is carried out here in the ^{208}Pb nucleus. In order to find out the shapes and strengths of the scalar and vector potentials from the numerical solution of the RMF equations for the spherical ^{208}Pb nucleus, following Koepf *et al* [15], the potentials $u(r)$ and $w(r)$ are fitted to the Woods-Saxon shapes.

$$u_{p(n)}(\mathbf{r}) = \frac{V^0_{p(n)}}{1+\exp\left(\frac{r-r_{p(n)}}{a_{p(n)}}\right)} \quad , \tag{19}$$

$$w_{p(n)}(\mathbf{r}) = \frac{-\lambda_{p(n)}V^0_{p(n)}}{1+\exp\left(\frac{r-r^{ls}_{p(n)}}{a^{ls}_{p(n)}}\right)} \quad . \tag{20}$$

The strength parameters $V^0_{p(n)}$ are taken to be smooth functions of protons (neutrons) $(Z(N))$.

$$V^0_{p(n)} = V\left(1 \pm \chi_{p(n)}\frac{N-Z}{N+Z}\right) \quad . \tag{21}$$

The radii $r_{p(n)}$ and $r^{\ell s}_{p(n)}$ having the well known A dependence.

$$r_{p(n)} = r_{0_{p(n)}}A^{\frac{1}{3}} \tag{22}$$

$$r^{\ell s}_{p(n)} = r^{\ell s}_{0_{p(n)}}A^{\frac{1}{3}} \quad . \tag{23}$$

The numerical values of the unknown parameters in the potentials of Woods-Saxon shape are obtained for the Lagrangian parameter set NL1 and are listed in Table 1. The scalar potential $s(= g_\sigma\sigma)$ and the vector potential $v(= g_\omega\omega)$ used in the solution of the Dirac equation are obtained by using equations (19) and (20).

$$\bar{\sigma} = s = \left[\frac{(u_p+u_n)-(w_p+w_n)}{4}\right] \tag{24}$$

$$\bar{\omega} = v = \left[\frac{(u_p+u_n)+(w_p+w_n)}{4}\right] \quad . \tag{25}$$

The potentials s and v calculated from Eqs. (19)-(20) for the ^{208}Pb nucleus are shown in Fig. 1.

From Table 1 it is to be observed that the relativistic (RMF) scalar and vector potentials for ^{208}Pb nucleus, have the Woods-Saxon shapes to very good accuracy. This can also visually be seen from the fit presented in the Fig 1. From Table 1 and equations (24) and (25) defining v and s it is to be observed that the strength of s and v are not equal, and they have opposite signs as expected. It is found that $v + 0.812s$ is zero. This curve is also shown in Fig. 1. For the purpose of variation of the vector field a parameter α is introduced through the relation $v = \alpha s$ within the range $-0.95 \leq \alpha \leq -0.6$. Here both v and s have the same shape. The Dirac equation is numerically solved for the values of α in the above range.

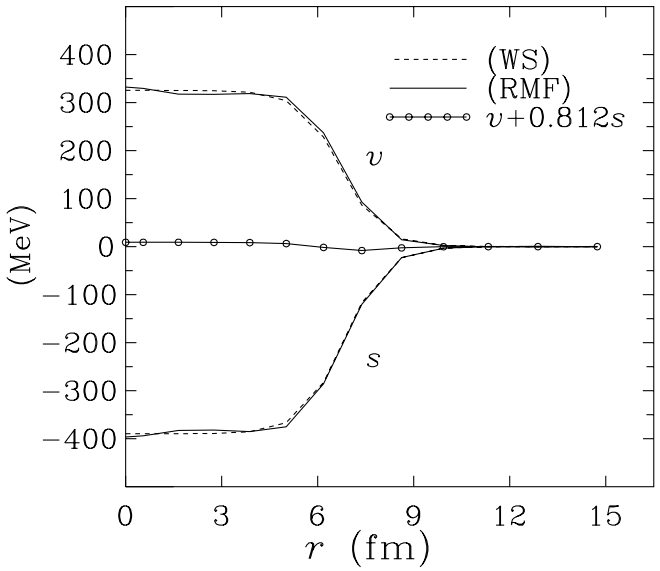

Fig. 1. The scalar potential s (MeV) and the vector potential v (MeV) for the nucleus ^{208}Pb

Table 1. Parameters of the Woods-Saxon potential for protons (p) and neutrons (n) [15]

	V (MeV)	χ	λ	r_0	a	r_0^{ls}	a^{ls}
				(fm)			
p	−71.28	0.462	8.97	1.25	0.612	1.14	0.647
n	−71.28	0.462	11.12	1.233	0.615	1.144	0.648

The variation of the calculated neutron (proton) single particle energies (MeV) with α are shown in Figs. 2 (3) for the ground state of ^{208}Pb. As seen from Figs. 2 and 3 all the bound single particle states are above the Dirac sea and are far away from zero in the relativistic situation. It is interesting to note that the valance levels bunch together and approach nearly zero value for α around -0.812 the realistic value. Further with the increase of α from the realistic value, more and more single particle states lie in the continuum.

The energy splitting $\Delta_{\rm ps}$ between pseudo-spin partners as a function of α is plotted in Fig. 4. It reveals that for realistic fields ($v \simeq -0.812s$), the splitting of the pseudo-spin partners of the Dirac bound valence states is very small compared to $\hbar\omega$ ($\simeq$ 7MeV). For example the unoccupied (particle) states show near degeneracy of the pseudo-spin partners $(4s_{1/2},\ 3d_{3/2})$ $(3d_{5/2},\ 2g_{7/2})$ and $(2g_{9/2},\ 1i_{11/2})$. In fact the maximum absolute value of the energy splitting of these pseudo-spin partners is less than 1MeV, except for $(2g_{9/2},\ 1i_{11/2})$ involving the intruder states where its value is close to -1.5MeV. The corresponding near degeneracy is also observed between the pseudo-spin partners for the hole states (proton particle states) $(3p_{3/2},\ 2f_{5/2})$, $(2f_{7/2},\ 1h_{9/2})$ and also for $(3s_{1/2},\ 2d_{3/2})$, $(2d_{5/2},\ 1g_{9/2})$. For example $\Delta_{\rm ps}(4s_{1/2},\ 3d_{3/2}) = \Delta_{\rm ps}(3d_{5/2},\ 2g_{7/2}) \simeq 0.0$ for $\alpha = -0.812$, $\Delta_{\rm ps}(3p_{3/2},\ 2f_{5/2}) \simeq 0.0$ for $\alpha = -0.845$, $\Delta_{\rm ps}(2f_{7/2},\ 1h_{9/2}) = \Delta_{\rm ps}(3s_{1/2},\ 2d_{3/2}) \simeq 0.0$

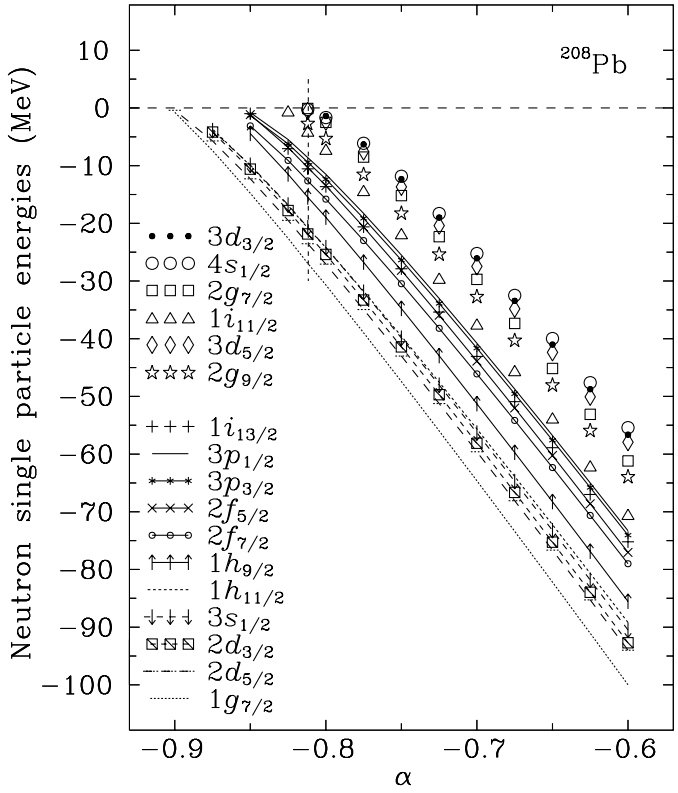

Fig. 2. The variation of the neutron single particle energies (MeV)

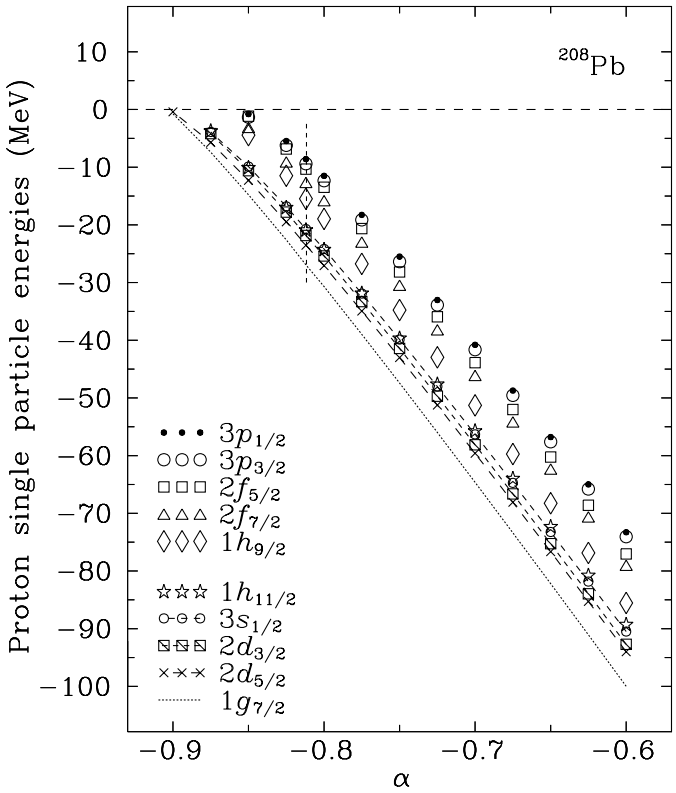

Fig. 3. The variation of the proton single particle energies (MeV)

for $\alpha = -0.90$ and $\Delta_{\rm ps}(2d_{5/2}, 1g_{7/2}) \simeq 0.0$ for $\alpha = -0.95$. Thus the near pseudo-spin degenerate pair of valence orbitals exist for the realistic value of α. Thus it is expected that the pseudo-spin doublets shown in the figure will be degenerate as $\alpha \to -1.0$ as remarked in [12]. Because in this case a strong repulsive potential v is used which nearly cancels the attractive potential s and therefore, all the states are close to the continuum.

The important observations from Fig. 4 are the following:

- The pseudo-spin splitting decreases with the increase in radial quantum number n for the physical value of $\alpha = -0.812$.
- The pseudo-spin symmetry is seen to occur near the Fermi surfaces of protons and neutrons in the ^{208}Pb nucleus and not close to the potential height.

The energy splitting $\Delta_{\rm ps}$ is smaller for higher value of n (higher excited) pseudo-spin partner states than that of the strongly bound (lower values of n) pseudo-spin doublets. This can be understood from the fact that the term that splits the pseudo-spin partners for a given $\tilde{\ell}$ has energy dependence $E+(s+v)$ (see (27)) in the denominator. For deeper lying states E is larger so the denominator becomes smaller in magnitude resulting in lerger pseudo-spin splitting for a given $\tilde{\ell}$.

It is known that spin orbit splitting plays an important role in the existence of pseudo-spin symmetry. And in view of the correct prediction of the spin orbit splitting in the RMF [9,16], we study its variation with the approachment towards the pseudo-spin symmetry limit. For this point of view the spin orbit splitting is plotted in Fig. 5 as a function of α. It is observed that for realistic value $\alpha = -0.812$, the spin orbit splitting is small (less than 2.5 MeV) except for the orbitals $(2g_{7/2}, 2g_{9/2})$.

In order to search for the observable that is sensitive to the occurrence of pseudo-spin symmetry the neutron (proton) root mean square radii $r_n(r_p)$ are calculated. Their variation with alpha is shown in Fig. 6. They are found to increase faster for $\alpha \leq -0.812$ while they vary slowly for $\alpha \geq -0.812$. This observation indicates the strong variation of the properties of the pseudo-spin partner orbitals with α for the values of $\alpha \ll -0.812$. In order to verify this point, the wave functions of the pseudo-spin partners are plotted in the Figs.7–14. The upper and lower components of the wavefunctions corresponding to different pseudo-spin partners for the values of α=−0.812 and α=−0.850 are shown in these figures. From these figures it is clear that the nodes of the radial wavefunctions f of the pseudo-spin partners differ by one unit as required by the orthogonality conditions. The f corresponding to the lower ℓ value having one node more than the f corresponding to $\ell + 2$. This type of behaviour is seen in all the cases studied here. It is found from these figures that the lower components g are small and are of almost equal in magnitude, with opposite signs. It is also seen that the nodal points of f shifts at larger distances as the values of α decrease from −0.812 to −0.850. It is an important

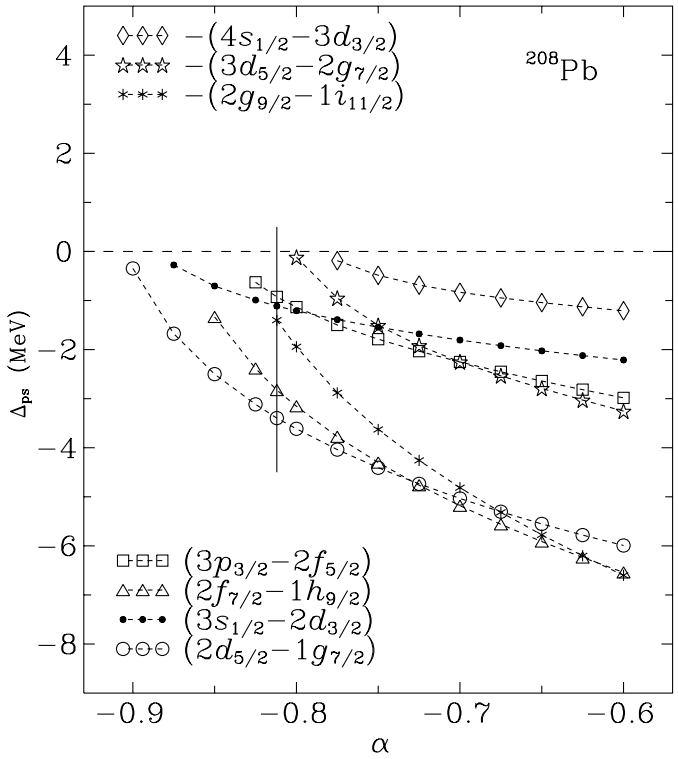

Fig. 4. The variation of the energy splittings $\Delta_{\rm ps}$ (MeV) between the pseudo-spin partners for the nucleus ^{208}Pb with α

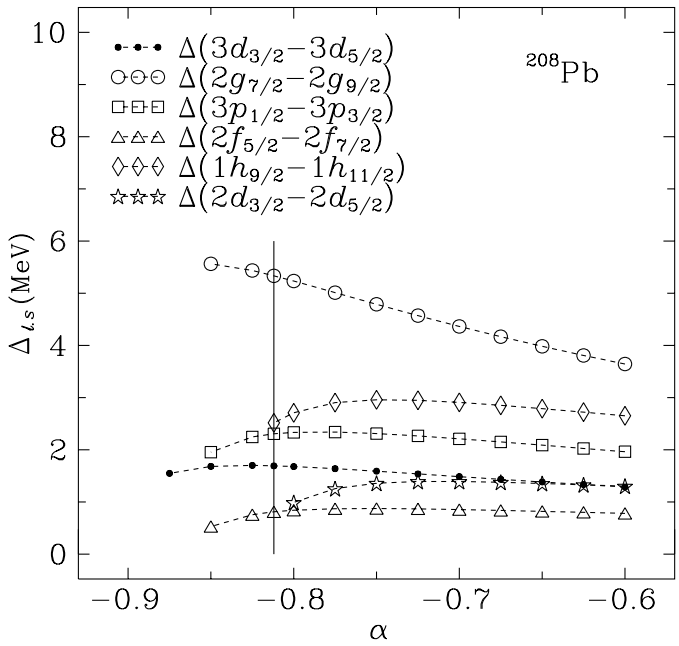

Fig. 5. The variation of the spin orbit splittings (MeV) for the nucleus ^{208}Pb with α

observation that the lower component g approaches zero as $\alpha \rightarrow -1.0$. It indicates that the orbit radii increase for larger repulsive potential for the same attractive part i.e., for $v+s$ approaching zero. Some of these observations were also noticed in [17].

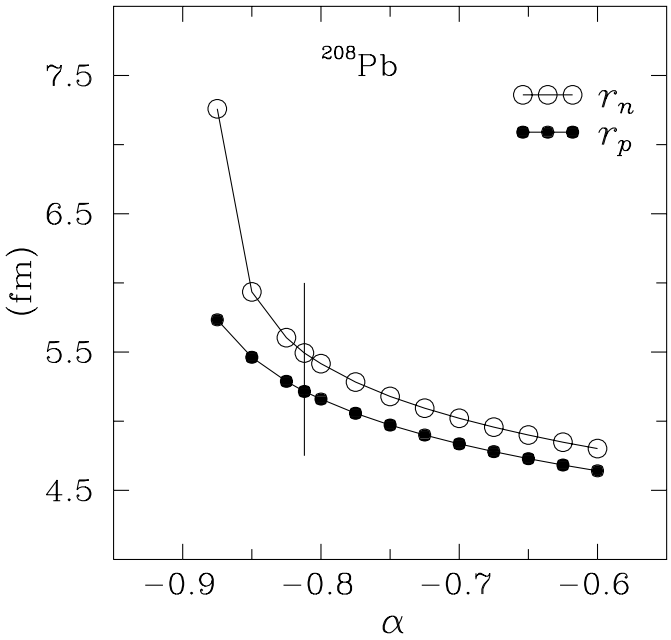

Fig. 6. The variation of the point neutron (r_n), proton (r_p), root mean square ($r_{\rm rms}$) radii (fm) for the nucleus ^{208}Pb with α

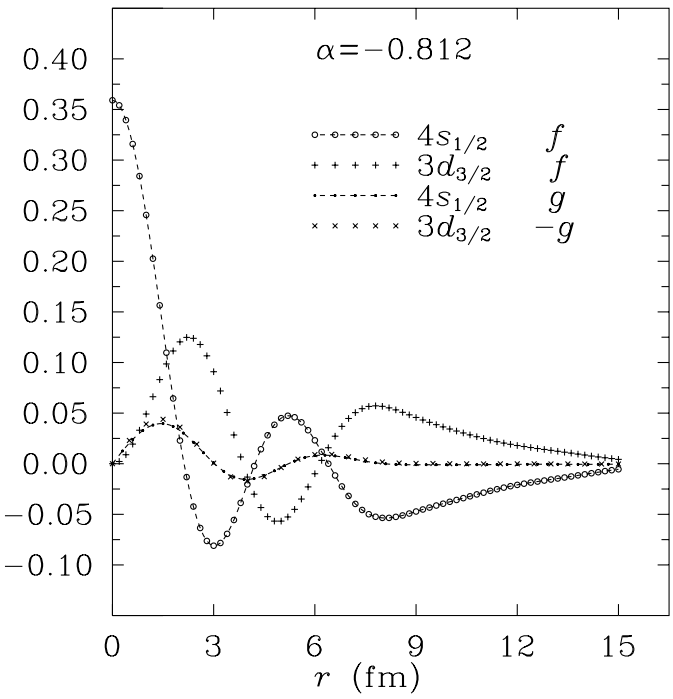

Fig. 7. Dirac spinors f and g of the pseudo-spin partners $4s_{1/2}$ and $3d_{3/2}$ for the nucleus ^{208}Pb for $\alpha = -0.812$

4 Some analytic properties

It is easy to obtain a second order differential equation for the lower component ψ_{ℓ_i} of ψ_i by eliminating the upper component ψ_{u_i} from (6). In the case of a spherical nucleus, the potentials $s(\mathbf{r})$ and $v(\mathbf{r})$ are functions only of the magnitude r. Therefore, this equation takes the fol-

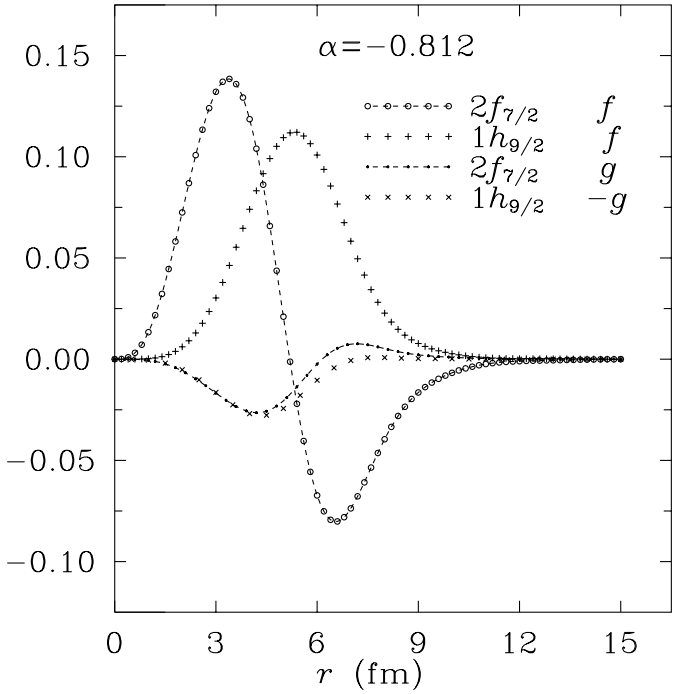

Fig. 8. Dirac spinors f and g of the pseudo-spin partners $2f_{7/2}$ and $1h_{9/2}$ for the nucleus ^{208}Pb $\alpha = -0.812$

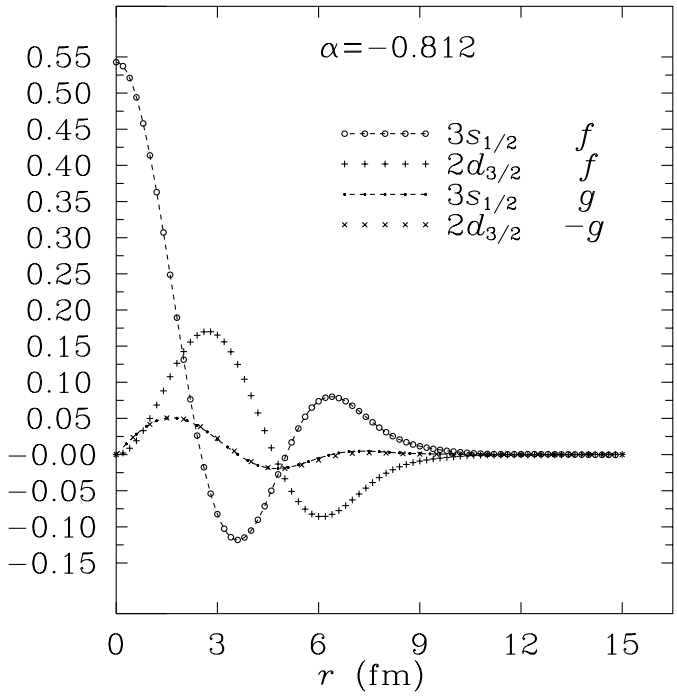

Fig. 10. Dirac spinors f and g of the pseudo-spin partners $3s_{1/2}$ and $2d_{3/2}$ for the nucleus ^{208}Pb $\alpha = -0.812$

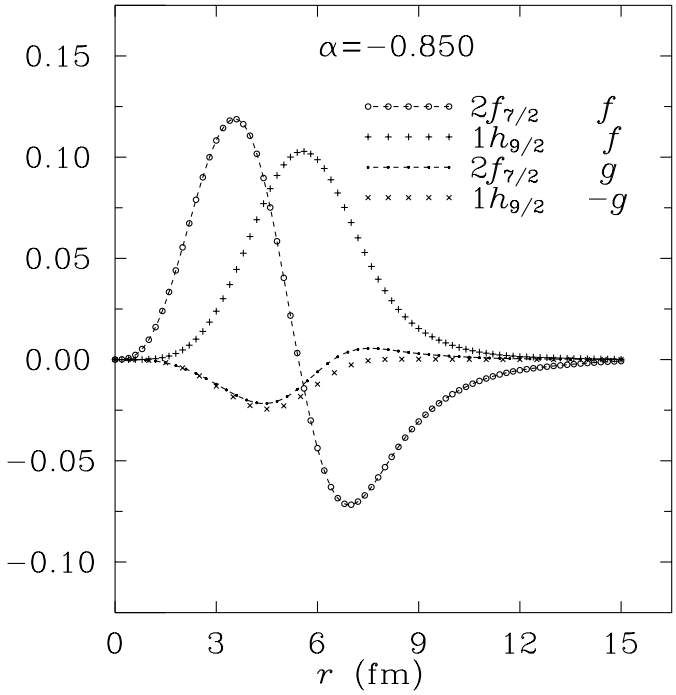

Fig. 9. Dirac spinors f and g of the pseudo-spin partners $2f_{7/2}$ and $1h_{9/2}$ for the nucleus ^{208}Pb $\alpha = -0.850$

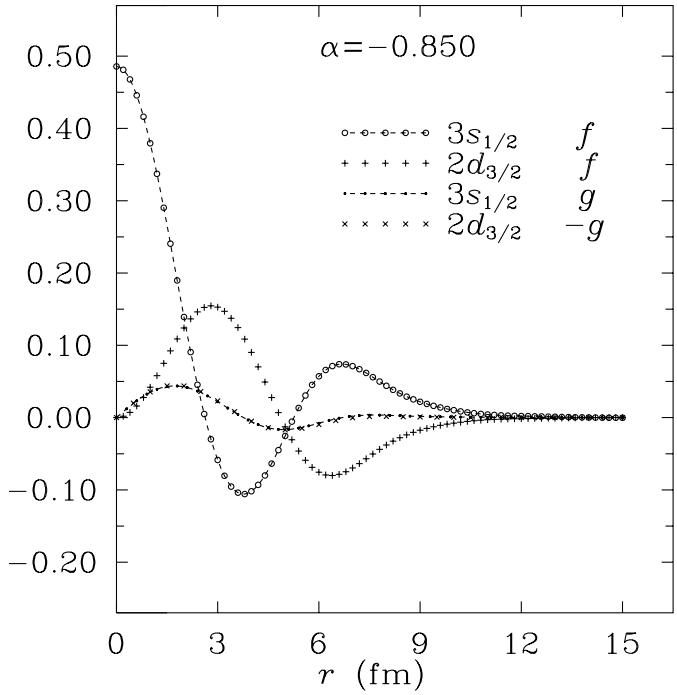

Fig. 11. Dirac spinors f and g of the pseudo-spin partners $3s_{1/2}$ and $2d_{3/2}$ for the nucleus ^{208}Pb $\alpha = -0.850$

lowing form:

$$\left\{-\nabla^2 + \frac{s'+v'}{(s+v)+E}\left(\frac{\partial}{\partial r} - \frac{1}{r}(\sigma\cdot\mathbf{L})\right)\right\}\psi_{l_i} = (2-E-(v-s))\,(E+(v+s))\psi_{l_i} \quad . \quad (26)$$

Using the definition $\hat{\kappa}\psi = -\beta(\Sigma\cdot\mathbf{L}+1)\psi = \kappa\psi$ one obtains the relations $\sigma\cdot\mathbf{L}\psi_{l_i} = (\kappa_i - 1)\psi_{l_i}$ and $\sigma\cdot\mathbf{L}\psi_{u_i} = -(\kappa_i+1)\psi_{u_i}$. The above equation can be written as

$$\left\{-\nabla^2 + \frac{s'+v'}{(s+v)+E}\left(\frac{\partial}{\partial r} - \frac{1}{r}(\kappa_i - 1)\right)\right\}\psi_{l_i} = (2-E-(v-s))\,(E+(v+s))\psi_{l_i} \quad . \quad (27)$$

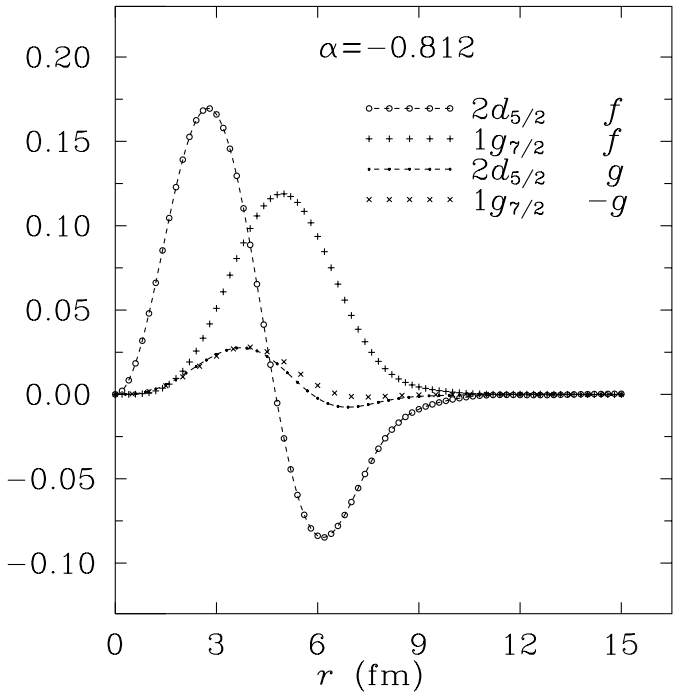

Fig. 12. Dirac spinors f and g of the pseudo-spin partners $2d_{5/2}$ and $1g_{7/2}$ for the nucleus ^{208}Pb $\alpha = -0.812$

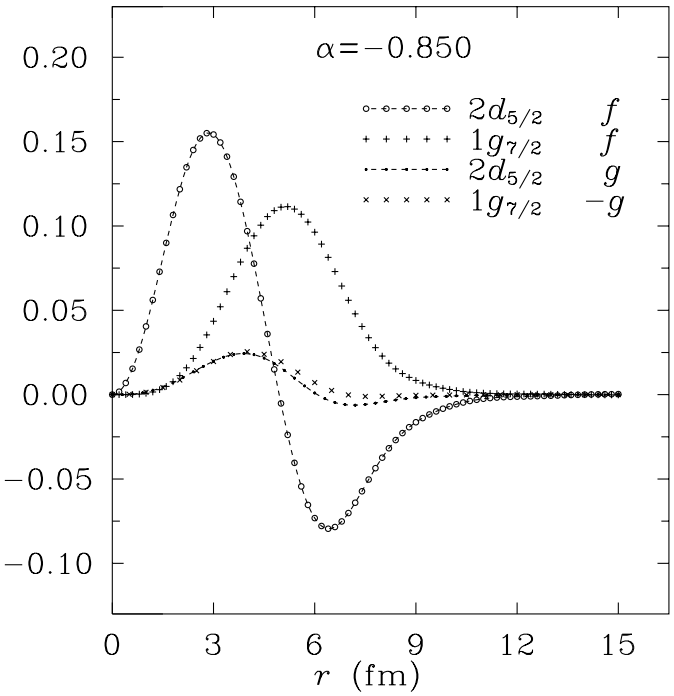

Fig. 13. Dirac spinors f and g of the pseudo-spin partners $2d_{5/2}$ and $1g_{7/2}$ for the nucleus ^{208}Pb $\alpha = -0.850$

Here s' (v') are the derivatives of s (v) with respect to (w.r.t.) r and the binding energy $E \geq 0$ measured w.r.t. the nucleon mass M in the natural units $\hbar = c = 1$. For the case of equal strengths, $s + v = 0$, the (27) reduces to:

$$-\nabla^2 \psi_{l_i} + E(v-s)\psi_{l_i} \;=\; E(2-E)\psi_{l_i} \quad . \tag{28}$$

Clearly (28) has energy dependent potential ($E(v-s)$) and has eigen value $E(2-E)$. After scaling the radial variable $r = x/(\sqrt{E})$, the potential has a complicated ($\sqrt{E}$) dependence *i.e.,* $-s\left(x/\sqrt{E}\right) + v\left(x/\sqrt{E}\right)$. In such a situation the (28) is not a normal Schrödinger eigen value equation. Further it is obvious that $E = 0$ solution of this equation exists and is not normalisable. Besides in that case all states are degenerate. This equation is the same as the (3) of [12] in the scaled variable x when written in terms of the partial waves and use is made of the relation $\ell(\ell+1) = \kappa(\kappa-1)$.

Similarly eliminating the lower component ψ_{l_i} we have for the upper component ψ_{u_i} the following second order differential equation,

$$\left\{-\nabla^2 - \frac{-s'+v'}{2-E-(-s+v)}\left(\frac{\partial}{\partial r} - \frac{1}{r}\sigma\cdot\mathbf{L}\right)\right\}\psi_{u_i} = -(E+(s+v))(2-(-s+v)-E)\psi_{u_i} \tag{29}$$

Using the relations obtained from the definition of $\hat{\kappa}$, this equation can be written in the form

$$\left\{-\nabla^2 - \frac{-s'+v'}{2-E-(-s+v)}\left(\frac{\partial}{\partial r} + \frac{1}{r}(1+\kappa_i)\right)\right\}\psi_{u_i} = -(E+(s+v))(2-(-s+v)-E)\psi_{u_i} \tag{30}$$

The first observation of the energy dependent (27) and (30) is that the spin orbit terms in these equations are proportional to the derivative factor ($\pm s' + v'$) corresponding to the lower and upper component second order equations. From the radial shapes of $s(r)$ and $v(r)$ seen in Fig. 1 it is clear that the spin orbit splitting is very sensitive to the shape of the nuclear surface region. It is nearly zero inside the nucleus and is sharply peaked in the surface region. In fact it is zero inside the nucleus for a square well potential shape and is non zero only on the nuclear surface. The pseudo-spin symmetry is seen to occur near the Fermi surfaces of protons and neutrons in ^{208}Pb nucleus and not close to the potential height.

5 Summary of the results

The possible existence of broken pseudo-spin symmetry in ^{208}Pb nuclei is investigated. The relativistic mean field approximation is made to the many body problem described by the Walecka Lagrangian. The parameters used are those which fit the ground state data of the Pb nucleus. Within this reliable many body frame work the existence of nuclear degenerate excited pseudo-spin partners are predicted. Surprisingly the radial parts of the lower

components of the Dirac spinors of these doublet states are of near equal magnitude (although very close to zero) and of opposite phase. The spin orbit RMF potential strongly peaks in the nuclear surface region, since its radial dependence has the expected factor $(s' + v')$, the derivative of the Woods-Saxon shape. Also its magnitude is small. In fact it is zero inside the nucleus for a square well potential and is non-zero only on the nuclear surface. This finding shows the strong RMF (nuclear) potential shape dependence of the existence of the broken pseudo-spin symmetry. The correlation between the energy separation of the doublet Δ_{ps} to the spin orbit splitting $\Delta_{\ell s}$ indicates that for the small values of the the doublet separation Δ_{ps} the spin orbit separation is small. For ^{208}Pb nucleus excited to the pseudo-spin symmetric state the root mean square neutron proton radii are found to be very sensitive to the deviation of the vector potential $v = \alpha s$ from $\alpha = -0.812$, the ground state value for the ^{208}Pb nucleus. They vary slowly for $\alpha > -0.812$ while they increase much faster for $\alpha <$ -0.812. This is the reflection of the sensitivity of the pseudo-spin symmetry phenomenon to the relative strength of the vector and scalar potentials and their shapes.

We thank J. N. Ginocchio for his correspondence relating to the structure of the wave functions. The financial support from the Department of Science and Technology (DST) Government of India is gratefully acknowledged.

References

1. K. T. Hecht, A. Adler, *Nucl. Phys.* **A137**, 129 (1969)
2. A. Arima, M. Harvey, K. Shimizu, *Phys. Letts. B* **30**, 517 (1969)
3. A. Bohr, I. Hamamoto, B. R. Mottelson, *Phys. Scr.* **26**, 267 (1982)
4. B. Mottelson, *Nucl. Phys.* **A522**, 1 (1991)
5. R. D. Ratna Raju, J. P. Draayer, K. T. Hecht; *Nucl. Phys.* **A202**, 433 (1973)
6. O. Castanos, M. Moshinsky, C. Quesne, *Phys. Letts. B* **277**, 238 (1992)
7. A. L. Blokhin, C. Bahri, J. P. Draayer, *Phys. Rev. Lett.* **74**, 4149 (1995)
8. A. L. Blokhin, C. Bahri, J. P. Draayer, *J. Phys. A* **29**, 2039 (1996)
9. C. Bahri, J. P. Draayer ans S. A. Moszkowski, *Phys. Rev. Lett.* **68**, 2133 (1992)
10. A. L. Blokhin, T. Beuschel, J. P. Draayer, C. Bahri, *Nucl. Phys.* **A612**, 163 (1997)
11. T. Beuschel, A. L. Blokhin, J. P. Draayer, *Nucl. Phys.* **A619**, 119 (1997)
12. J. N. Ginocchio, *Phys. Rev. Lett.* **78**, 436 (1997)
13. J. D. Walecka, *Ann. Phys. (N.Y.)* **83**, 491 (1974)
14. Y. K. Gambhir, P. Ring, A. Thimet, *Ann. Phys. (N.Y.)* **198**, 132 (1990), references cited therein
15. W. Koepf, P. Ring, *Z. Phys. A* **339**, 81 (1991)
16. B. D. Serot, J. D. Walecka, *Adv. Nucl. Phys.* **16**, 1 (1986)
17. J. N. Ginocchio, D. G. Madland; *Phys. Rev. C* **57**, 1887 (1998)